On Dynamic effects of Bulbous Bow Crushing

Chen, Jun ; Zhu, Ling; Pedersen, Preben Terndrup

Published in:
Proceedings of the 29th International Ocean and Polar Engineering Conference

Publication date:
2019

Document Version
Publisher's PDF, also known as Version of record

Proceedings of the Twenty-ninth (2019) International Ocean and Polar Engineering Conference **www.isope.org**
Honolulu, Hawaii, USA, June 16-21, 2019

ISBN 978-1 880653 85-2; ISSN 1098-6189

On Dynamic effects of Bulbous Bow Crushing

Jun Chen[1,2]，Ling Zhu [1,3]，Preben Terndrup Pedersen[4]
[1]. Departments of Naval Architecture, Ocean and Structural Engineering, School of Transportation, Wuhan University of Technology, Wuhan, P.R. China
[2]. Key Laboratory of High Performance Ship Technology of Ministry of Education, School of Transportation, Wuhan University of Technology, P.R. China
[3]. Collaborative Innovation Centre for Advanced Ship and Deep-sea Exploration, Wuhan, China
[4]. Department of Mechanical Engineering, Technical University of Denmark, Lyngby, Denmark

ABSTRACT

For evaluation of the consequences of ship-ship collisions, and ship collisions against offshore installations and bridges, it is important to know the force-displacement relation and the energy absorption caused by crushing of complex bulbous bow structures. This paper presents a method to calculate the dynamic bow crushing forces using simplified analytical procedures taking into account the variation of the crushing velocity during impact. Firstly, a non-linear finite element method is applied to simulate the dynamic as well as the quasi-static crushing process of the large scale quasi-static bow crushing experiments performed by Yamada and Endo (2005). The dynamic crushing force-displacement relations, the strain rates and the energy absorption of the bow models are evaluated. An empirical relation is derived between the actual crushing velocity and the strain rates in the bow structure. For different ship impact velocities and impact masses, the dynamic impact results are compared with the experimental static crushing results. It is observed that for realistic velocities and masses the crushing forces and energy absorption of the bulbous bow structure is increased significantly due to the dynamic effects. Secondly, an analytical procedure is presented which is based on a quasi-static simplified calculation method modified by the derived relation between actual deformation velocity and the strain-rates. The varying crushing velocity is determined by an energy based procedure to give consistent estimates of the dynamic bow crushing forces. Finally, the simulated numerical non-linear finite element dynamic and static crushing responses are compared with the results of the presented simplified analytical method.

KEY WORDS: ship collision; crushing force; bulbous bow; dynamic and static crushing; finite element method; simplified analytical method.

INTRODUCTION

In ship collision analyses, the structural behavior of the bow plays a dominant role. For ship-ship collisions, it is the strength of the colliding bow which determines whether the energy will be absorbed primarily by the bow of the colliding ship or by structural damage to the struck vessel. In collisions with offshore structures, the designers will normally aim for a strength design of the installation such that the ship bow shall absorb most of the energy released for crushing. Similarly, in the structural design of bridges against ship collisions, the pylons and the bridge piers have to be designed to withstand bow impacts of the design vessels.

For studies of the bow crushing forces, quasi-static analytical simplified methods are widely used to evaluate the collision force. In order to simplify the structure and facilitate the study, the cross section of the bow is normally divided into three basic units as shown in Fig. 1: X, L, and T sections. Amdahl (1983) and Yang and Caldwell (1988) studied the mean crushing force of these different elements using the upper bound theorem. In order to further study these basic units, many researchers have carried out a large number of quasi-static crushing tests of square tubes and circular tubes, and the calculation formula for the mean crushing force is corrected by the test results. Wierzbicki and Abramowicz (1983), Abramowicz (1994) and Jones (1989) investigated the crushing force, folding mode and folding length in detail for these three basic elements. They presented analytical expressions based on their experimental results. For ship structures, it is convenient to predict the force of the entire bow structure by calculating the force of each basic unit and then sum the results for all the units. Lehmann and Yu (1995) developed a calculation method for the crushing force of a conical shell, which introduced the influence of the inclination angle. Paik and Pedersen (1995) proposed a method for predicting the crushing force using the individual plates as basic units. In this method, the mean crushing force of the plate element is obtained under two different boundary conditions (fix-free and fix-fix). Endo and Yamada (2005) simulated the quasi-static crushing process of conical bow models by experimental and numerical methods.

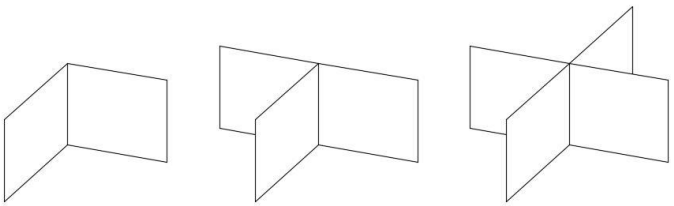

L-section T-section X-section
Fig.1. Sketch of three basic units

Pedersen et. al. (1993) applied the results of the model tests to verify

the methods of Amdahl (1983) and Yang and Caldwell (1988) and evaluated the collision forces with bulbous bows of six different ice strengthened vessels. An empirical formula for calculating the maximum collision force was derived. The method takes into account the effects of speed, mean strain rate, and ship loading. In order to predict the damage of the striking ship and the struck ship, Lützen (2000) compared the resistance of the longitudinally and transversely stiffened bows, and smaller crushing forces were found for the transversely stiffened bows. Zhang et. al.(2004) proposed a semi-analytical method to evaluate the crushing force and damage extent of the shipbow.

For normal strength design of structures, the yield and tensile strength of materials are based upon characteristic values which are around the 5% percentile of the probability distribution of the mechanical tests. As shown by Storheim and Amdahl (2015), the mean value of the yield stresses is much higher than these minimum requirements, about +20% for HT36 and +34% for mild steels, and the mean value of the tensile strength is also much higher than the minimum requirements, about +12% for HT36 and +14% for mild steels. It is shown that such material values should be used in bow crushing analysis in order to have realistic bow crushing forces.

Another factor which must be taken into account in evaluation of bow crushing forces is the effect of strain rates. High-speed impact tests of square tubes were conducted by Yoshitake et. al. (1998) with a speed of 11 m/s, and the effect of strain rates was confirmed to be huge during the dynamic crushing process. Collisions are by nature dynamic and it is well known that strain rates will increase the initial yield stress and the work hardening of steel. Numerous tests have been conducted on the effect of strain rates related to high speed ballistic impacts with strain rate of several hundred s^{-1}. For such high speed deformations, two effects appear: local inertia effects will play a role for the structural behavior and the effect of the strain rate on the yield stress is considerable. In the case of ship collisions, the velocities are much more modest. As will be shown in this paper the strain rates will typically be around 3-15s^{-1}. In this case, inertia effects play a very minor role but the strain rate effect should not be neglected.

Therefore, a study of the effect of strain-rate hardening on bow crushing forces will be presented first numerically and secondly it is indicated how the numerically derived relations between the varying impact velocities and the associated strain rates can be applied to derive a consistent practical simplified calculation procedure which includes the effect of the varying strain rate during the impact process.

FEM MODEL AND MATERIAL OF THE BULBOUS BOW

The finite element simulation is carried out by using the three large scale bulbous bow models in Yamada and Endo's (2005) research. In this paper, the section with the cruciform web is chosen for analysis. The model dimensions are shown in Fig. 2. The outer shell of the model is a conical shell structure, and the internal webs are in the form of a cruciform. The thickness of the outer shell is 10mm and the thickness of the web is 7mm as shown in Fig. 3. A non-linear finite analysis is applied to simulate the static crushing and the results of this FEA is compared with the results of quasi-static crushing experiment. Secondly, the model is dynamically crushed, considering three different speeds of 4m/s, 6m/s and 8m/s. Three different rigid board masses of 300t, 400t and 500t are also included. The crushing of the bow model is simulated by the ABAQUS program. Both the static and the dynamic crushing procedures are analyzed by using the rigid board to impact the bow structure. As shown in Fig. 4, the bottom surface of the conical shell is taken to be rigidly fixed, and the rigid board is given a motion in the negative direction of the Y axis. The initial speed of the movement is controlled in the dynamic crushing process and the displacement of the rigid board is controlled in the static crushing process. The finite element mesh size is 0.05m.

In the final section of the paper the simplified method is modified to calculate analytically the dynamic mean crushing force as function of the decreasing impact velocity. This is done by considering the effect of strain rate on the yield stresses.

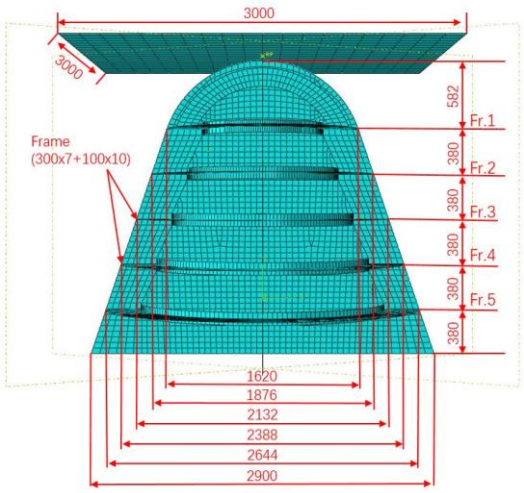

Fig. 2. Bulbous bow model by Yamada & Endo (2005)

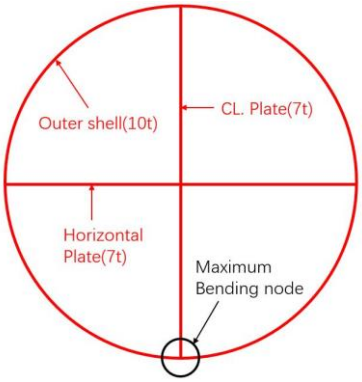

Fig. 3. Cross-section of the cruciform web

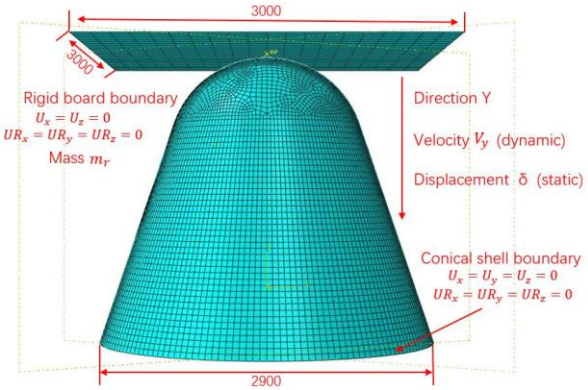

Fig. 4. Set-up of the FE model

The material is mild steel, and the applied material parameters are the results of standard tensile tests. The true stress-strain curve is shown in

Fig. 5 and the material properties are listed in Table 1. From the study of Paik and Thayamballia (2003), it was concluded that for analytical simplified analyses the flow stress is half the sum of yield strength and ultimate strength. This assumption has been shown to give a good estimation in the actual situation. Thus, the flow stress can be defined as:

$$\sigma_0 = \frac{\sigma_y + \sigma_u}{2} \tag{1}$$

where: σ_y is the yield stress; σ_u is the ultimate strength; σ_0 is the static flow stress.

The strain rate effect is considered in the following dynamic crushing analysis, and the Cowper-Symonds (1957) empirical formula is used to correct the material parameters:

$$\frac{\sigma_d}{\sigma_o} = 1 + \left(\frac{\dot{\varepsilon}}{D} \right)^{1/q} \tag{2}$$

where: σ_o is the static flow stress; σ_d is the dynamic flow stress; $\dot{\varepsilon}$ is the strain rate. The parameter D for mild steel is 40.4 and q is 5.

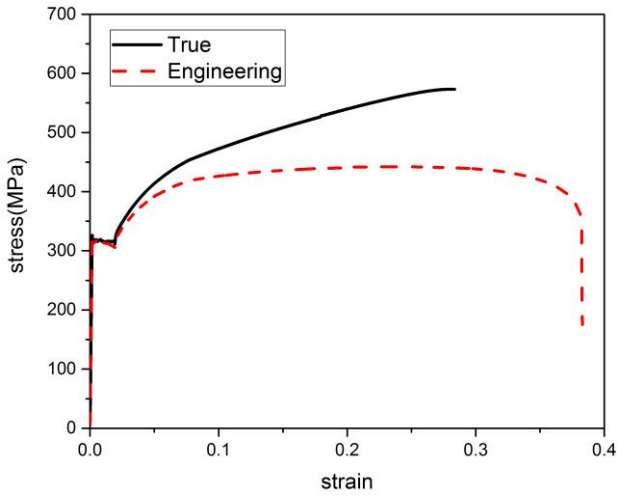

Fig. 5. Stress-strain curve of material tensile test

Table 1. Mechanical properties of the material

Property	Units	Magnitude
Young's modulus	Gpa	191
Poisson's ration	-	0.3
Mass Density	kg/m^3	7850
Yield stress	Mpa	313
Ultimate strength	Mpa	573

SIMPLIFIED STATIC ANALYSIS METHOD

In this paper, the applied method for the simplified analytical calculation of the mean crushing force is a combination of the methods of Wang (1995) and Lehmann and Yu (1995). Wang (1995)'s method is to divide the cross-section of the bow into three different basic units of L, T and X element. The mean crushing force of each unit is calculated and then integrated on the whole contact face. The formula of the mean crushing force is expressed as:

$$P_m^{'} = \alpha_I \alpha_E \sigma_0 A \tag{3}$$

Where: $\alpha_I = \dfrac{1 - \sqrt{\sin^2\theta + \frac{1}{9}\cos^2\theta}}{\frac{2}{3}\cos\theta}$

$\alpha_E = \dfrac{1.88}{\beta^{0.5}} + \dfrac{0.375}{\beta}$ for X element, $\alpha_E = \dfrac{0.87}{\beta^{0.5}} + \dfrac{2.51}{\beta}$ for T element

$\beta = \dfrac{b}{t}$, b is the breadth of the flange, t is the thickness of the plate; σ_0 is the flow stress; A is the sectional area; θ is the inclination angle of element from the crushing direction.

Here the method of Wang (1995) is used for calculating the crushing force of the inner webs of the structure. The resulting force is reduced according to the ratio of the sectional area. The formula is as follows:

$$P_m^{''} = P_m^{'} \times A_{web} / A_{web+shell} \tag{4}$$

The method of Lehmann and Yu (1995) is used to calculate the mean crushing force of the outer shell. This method is applicable to the transversely stiffened outer structure, and the influence of the inclination angle is considered in the calculation. In this paper, the method is used to calculate the crushing force of each shell segment. The formula for calculating the mean crushing force is as follows:

$$P_m^{'''} = 2.09\sigma_0 t^2 \left[\frac{2\pi R_i}{L} + \frac{L}{t} + (\pi + 2\varphi)\tan\varphi + 1 \right] \tag{5}$$

where: σ_0 is the flow stress; t is the thickness of the plate; L is the frame distance; R_i is the effective radius; φ is the conical angle.

The static mean crushing force of the combination of webs and shell segments is obtained by summation of the results from the two procedures:

$$P_m^s = P_m^{''} + P_m^{'''} \tag{6}$$

RESULTS AND DISCUSSION

Different mesh sizes have a large influence on finite element results. For the model in this paper, the mesh size effect on the crushing force is important, so here different mesh sizes are included for analysis. The mesh sizes are 25mm, 40mm, 50mm, 100mm, 150mm, 200mm, 250mm, as shown in Fig. 6. It can be seen that the force changes with the mesh size. When the mesh size is 100mm, 150mm, 200mm,250mm, the crushing force is becoming larger. The convergence result is obtained when the mesh size is between 25mm and 50mm. Considering the calculation time, The time is longer as the mesh size becomes smaller. So the mesh size of 50mm is accepted as optional.

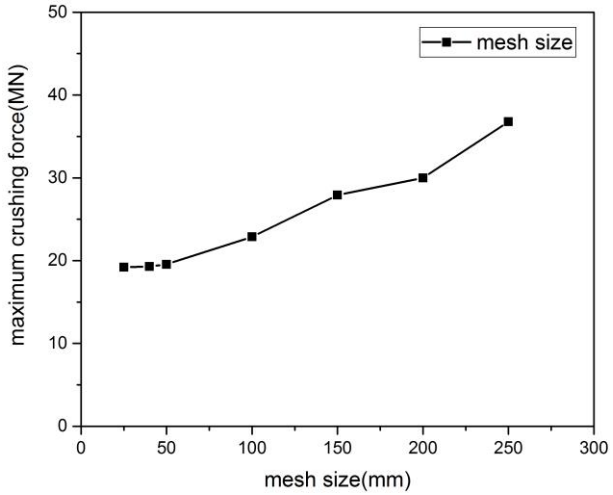

Fig. 6 Crushing force for different mesh sizes

The finite element simulated static and dynamic crushing processes are shown in Fig. 7. The quasi-static displacement of the rigid board is 1.96m and a total of 4 folds occurred, see Fig. 7(a). It can be seen that the bending strain is largest at the folds. For the process of dynamic crushing, there are two different non-linear finite element studies. Firstly, the mass of the rigid board is 500t, and the impact speed is 4m/s, 6m/s and 8m/s. Secondly the initial speed of the rigid board is set as 8m/s and the mass is changed between 300t, 400t and 500t. The crushing force, strain rate and energy absorption are evaluated for all these load cases.

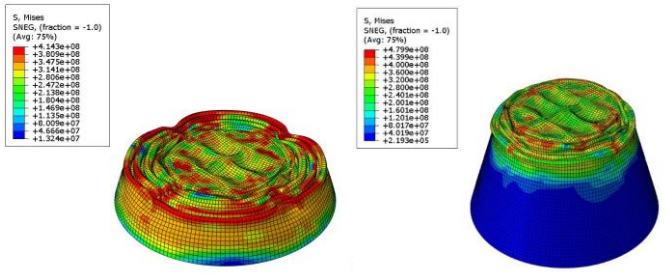

(a) Static crushing (b) Dynamic(V=8m/s,m=300t)

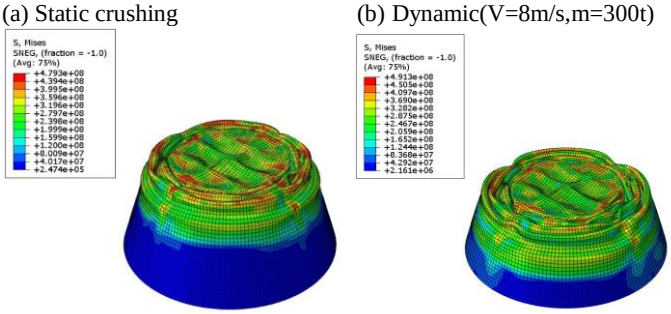

(c) Dynamic(V=8m/s,m=400t) (d) Dynamic(V=8m/s,m=500t)

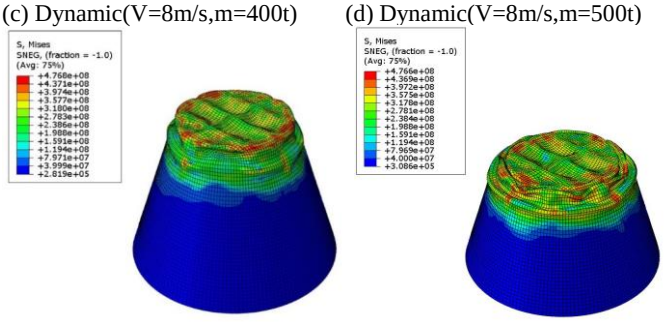

(e) Dynamic(V=4m/s,m=500t) (f) Dynamic(V=6m/s,m=500t)

Fig. 7. Deformation for static and dynamic crushing by FEA(stress units: Pa)

The purpose for the comparison between the FE static results and the static experiment is to verify the applied numerical FE model. For the three different impact speeds, the relationship between the crushing force and displacement is shown in Fig. 8. For the three different masses of the rigid board, the relationship between the crushing force and displacement is shown in Fig. 9. It can be seen from the figures that the initial dynamic crushing force is significantly larger than the static crushing force. Due to the influence of the strain rate, the crushing force will become significantly larger as the initial speed increases, and the total displacement will also increase greatly. For the same impact velocity but with increasing mass, the change of crushing force is not significant, but the total displacement is different due to the difference in the amount of energy to be absorbed.

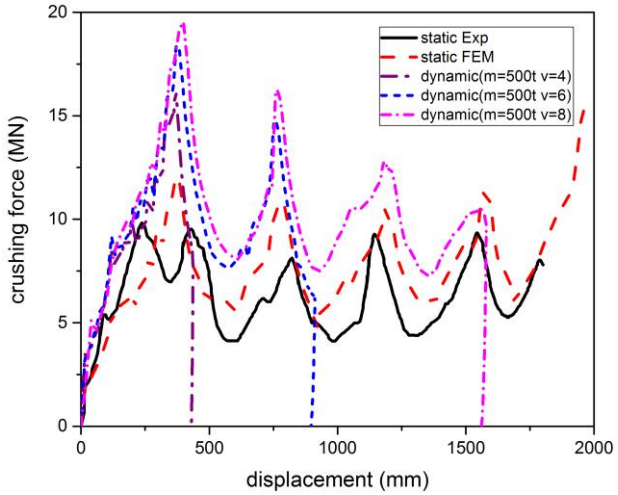

Fig. 8. Crushing force-displacement curve at different speeds

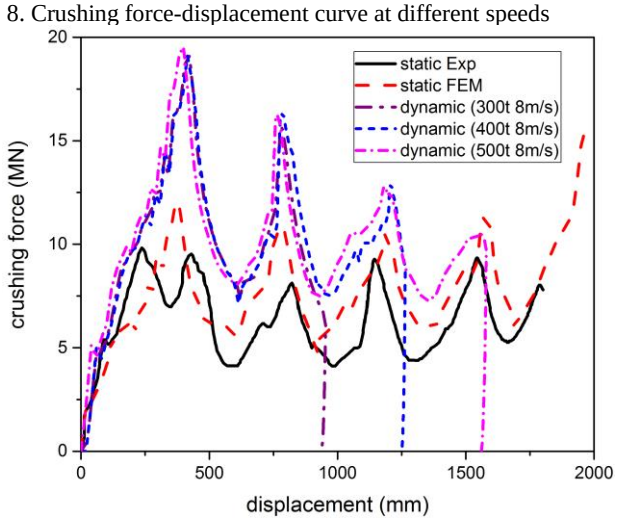

Fig. 9. Crushing force-displacement curve at different masses

From Figs. 8 and 9 it is noticed that the difference between the static and the dynamic crushing forces is large at the start of the impact and then reduced as the impact velocity is reduced near the end of the crushing process.

Since the conical outer shell structure is locally reinforced at the position of the transverse stiffeners, the maximum bending occurs at the elements between the transverse stiffeners. The nodes with the largest bending deformation at the three different speeds are shown in

Fig. 10. It can be seen from the Fig. 3 that the maximum strain occurs at the junction of the outer shell unit and the inner longitudinal member.

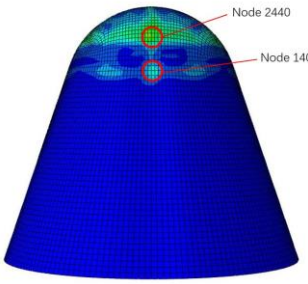

(a)m=500t,V=4m/s

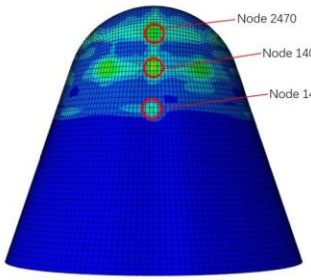

(b)m=500t,V=6m/s

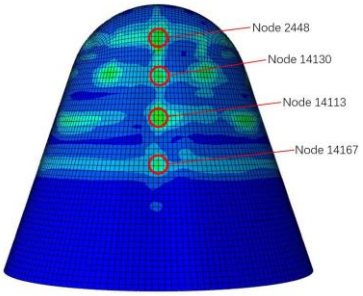

(c)m=500t,V=8m/s

Fig. 10. Position of maximum strain

The bending strain and displacement at these nodes which changes with the collision time are shown in Fig. 11. It can be observed that the strain and displacement of the nodes where the maximum bending occur increases with the collision time. The process can be considered to be nearly linear, and the slope of the curve is the corresponding strain rate and velocity. Since the collision time is short, the speed can be approximated as the average value and the strain rate is the equivalent average strain rate.

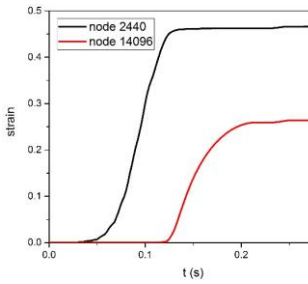

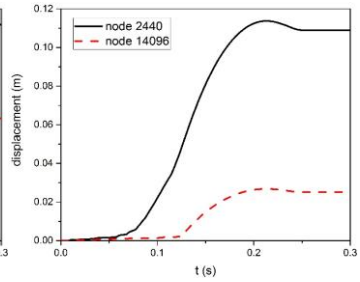

(a)strain-time curve at V=4m/s (b)Displacement-time curve at V=4m/s

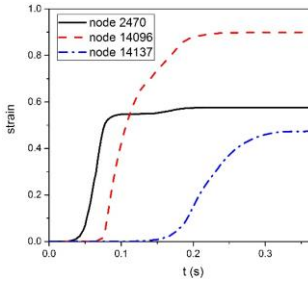

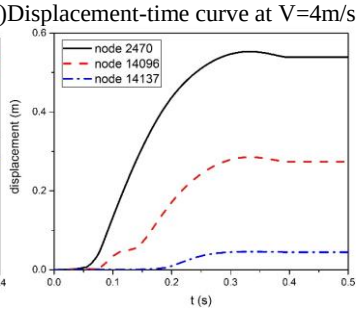

(c)strain-time curve at V=6m/s (d)Displacement-time curve at V=6m/s

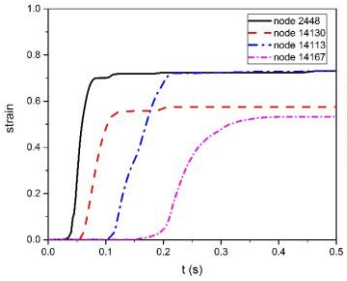

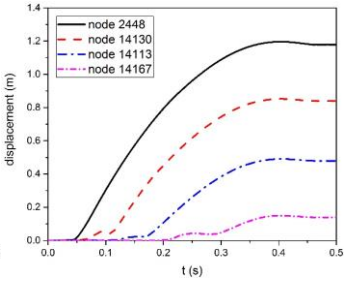

(e)strain-time curve at V=8m/s (f)Displacement-time curve at V=8m/s

Fig. 11. Strain and displacement-time curve at different velocities

Jones (1989) derived expressions for mean crushing forces for circular tubes. The ratio between the mean force for dynamic and quasi-static crushing was expressed:

$$\frac{P_m^d}{P_m^s} = 1 + \left(\frac{V}{4RD}\right)^{\frac{1}{q}} \tag{7}$$

where: P_m^d is the dynamic mean crushing force; P_m^s is the static mean crushing force; V is the initial velocity; R is the radius of the circular tube.

For the present conical bow structure, it is necessary to build a new relationship between the velocity V, the effective radius R_i and the strain rate $\dot{\varepsilon}$ at which the bending deformation occurs. Effective radius R_i is the radius at each frame shown in Fig.2. The average velocity of the nodes, the effective radius and equivalent average strain rate are listed in Table 2. It should be noted that the calculated strain rate depends on the mesh size. By analyzing the data in the table, a relationship is obtained as shown in Fig. 12. The data points are fitted to establish the relationship between the average strain rate and the ratio between the average velocity and the effective radius. The result of the curve fitting is as follows:

$$\dot{\varepsilon}_m = K\left(\frac{V_m}{R_i}\right)^n \tag{8}$$

where: K=4.41 and n=0.72. V_m is the mean velocity; R_i is the radius of i-th frame; $\dot{\varepsilon}_m$ is the average strain rate.

Table 2 Velocity, radius and strain rate of the maximum bending nodes

	Node	V_m（m/s）	R_i（m）	V_m / R_i	$\dot{\varepsilon}_m$
V=4 m/s	14096	0.2787	0.8431	0.3306	3.12
	2440	0.9143	0.67	1.3646	6.85
V=6 m/s	14137	0.2835	0.971	0.292	2.75
	14096	1.323	0.8431	1.57	6.64
	2470	2.303	0.7	3.29	9.9
V=8 m/s	14167	0.7845	1.1146	0.7038	2.87
	14113	2.3507	0.9867	2.3824	7.12
	14130	3.1	0.8588	3.6097	10.03
	2448	3.4758	0.7263	4.7856	14.21

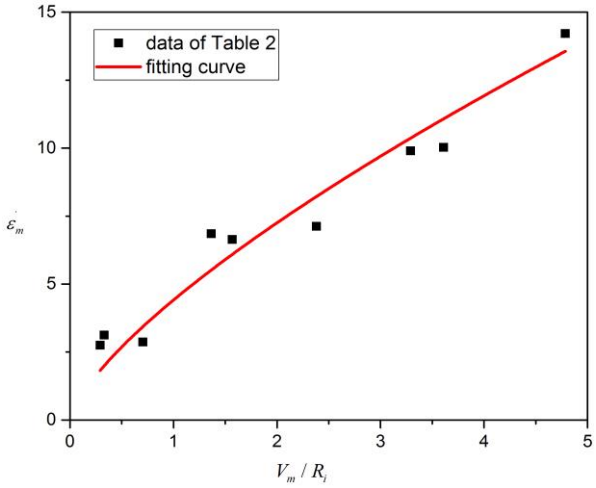

Fig. 12. Curve fitting between mean strain rate and the ratio of average crushing velocity to effective radius

SIMPLIFIED DYNAMIC ANALYSIS METHOD

From the analysis presented above, it is seen to be important to take into account the variation of the collision speed in order to get a realistic estimate of the strain-rate and the dynamic flow stress σ_d. To include this effect in a simplified analytical solution procedure, the energy dissipation during the collision can be considered in order to estimate the reduction of the collision speed during the collapse process.

Firstly the mean static crushing force is calculated for the sections between each frame in the bow. This can be performed by using a procedure such as the one expressed by Eqs. 3 to 6 or by use of one of the procedures tested by Yamada and Pedersen (2008). Applying Eq. 8 together with Eq. 1 and 2, the relation between the dynamic crushing force and the static crushing force can be expressed as:

$$\frac{P_m^d}{P_m^s} = \frac{\sigma_d}{\sigma_0} = 1 + f\left(\frac{V_m}{R_i}\right)^{n/q} \tag{9}$$

where: $f = \left(\frac{K}{D}\right)^{1/q}$

The initial kinetic energy E_0 of the striking ship is expressed as:

$$E_0 = 0.5MV_0^2 \tag{10}$$

where: V_0 is the initial velocity, M is the mass of the ship plus added mass in surge.

The kinetic energy E_1 after collapse up to the first frame will then be determined by

$$E_1 = E_0 - \delta \times P_{m,1}^s \times (1 + f(\frac{V_1}{R_1})^{n/q}) = 0.5MV_1^2 \tag{11}$$

where: $\delta = 0.75L$ is the effective crushing distance, L is the frame distance, V_1 is the velocity after collapse up to the first frame, R_1 is the effective radius of the first frame, $P_{m,1}^s$ is the quasi-static mean collision force up to the first frame.

From the energy balance Eq. 11, the mean velocity V_1 after the collapse up to the first frame can be determined and the associated collapse force $P_{m,1}^d$ can be found from Eq. 9. Using this procedure step by step, the energy balance for crushing of the subsequent bow sections is expressed as:

$$E_i = E_{i-1} - \delta_i \times P_{m,i}^s \times (1 + f(\frac{V_i}{R_i})^{n/q}) = 0.5MV_i^2 \tag{12}$$

where: V_i is the velocity at the actual indentation, $P_{m,i}^s$ is the quasi-static mean compression force at this indentation, δ_i is the effective crushing distance at this indentation, R_i is the effective radius of the i-th frame, E_i is the kinetic energy of the vessel after collapse of the bulb up to the considered frame, E_{i-1} is the kinetic energy at the previous frame.

Using Eqs, 9 and 12, the iteration can continue until the energy becomes negative and all the initial kinetic energy is absorbed by crushing of the bulbous bow. Thus the dynamic mean force at each frame is as follows:

$$P_{m,i}^d = P_{m,i}^s \times (1 + f(\frac{V_i}{R_i})^{n/q}) \tag{13}$$

Using the above formulas, the crushing velocities at each frame can be obtained and then the dynamic mean force $P_{m,i}^d$ at each frame can be calculated for the simplified dynamic method. Fig. 13 shows the resulting dynamic mean crushing forces obtained by the presented simplified dynamic procedure. Included in Fig. 13 is the results from the non-linear finite element calculations. It can be observed from these curves that the dynamic mean crushing force will fall down at the maximum displacement and become equal to the static mean force because the speed approaches zero at the end of the collision.

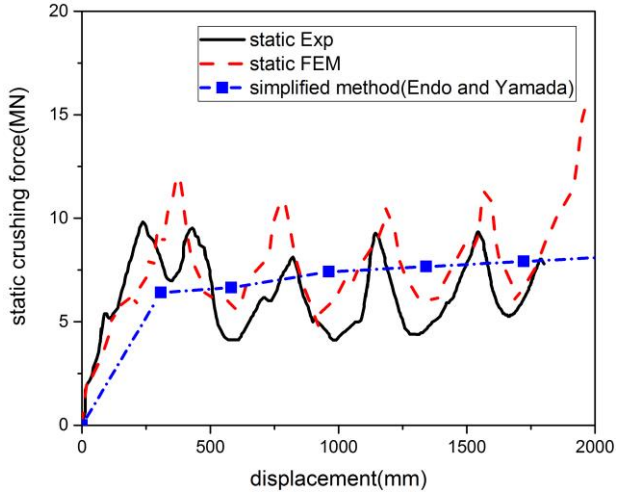

(a)Static crushing force-displacement curve by Yamada and Endo(2005)

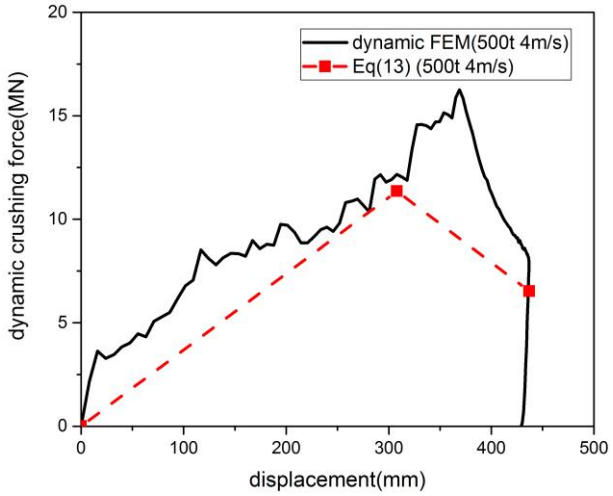

(b)Dynamic crushing force-displacement curve and analytical dynamic mean crushing force at 4 m/s

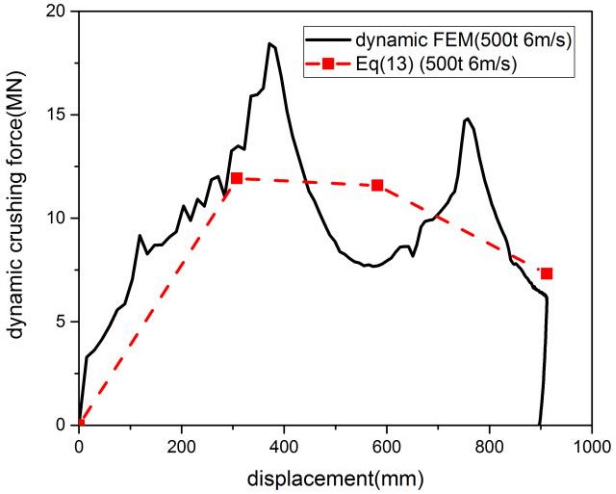

(c)Dynamic crushing force-displacement curve and analytical dynamic mean crushing force at 6 m/s

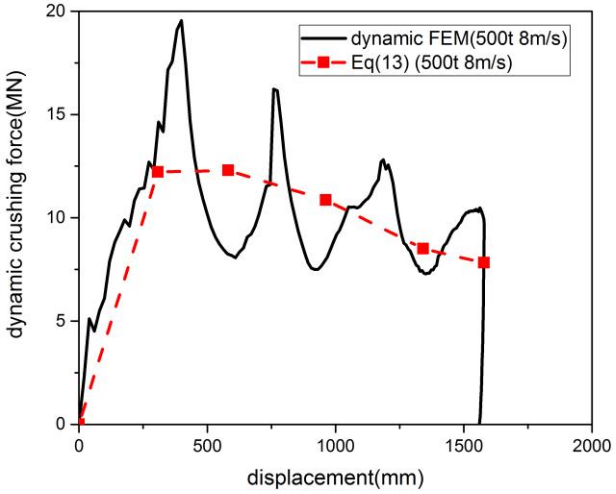

(d)Dynamic crushing force-displacement curve and analytical dynamic mean crushing force at 8 m/s

Fig. 13. FEM results of dynamic crushing force-displacement curve and simplified analytical dynamic mean crushing force at different velocities

From the perspective of energy absorption, the analytically determined dynamic crushing energy is compared with the FEM result. The comparison is shown in Fig. 14. It can be concluded that the results of energy obtained by the modified formulas is smaller than the dynamic crushing results of finite element method, but is larger than static condition. Especially when the displacement is small, the difference is obvious. The main reason for this is that the applied simplified analytical formulas for the static crushing force at small displacements give too low values.

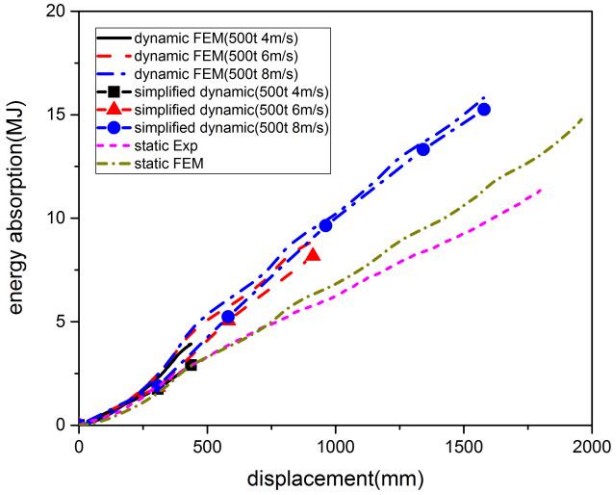

Fig. 14. Energy absorption-displacement curve of static and dynamic crushing by FEM and the simplified analytical formula

CONCLUSION

The purpose of this paper is to present a consistent method to calculate the dynamic bow crushing forces using simplified analytical procedures taking into account the variation of the crushing velocity during impact. Firstly, non-linear finite element simulations of a model of a bulbous bow is carried out, and the results of static crushing test are used to verify the static finite element results to make sure that the modelling and the material properties are suitable for the following investigation. Dynamic simulations of the bow structure crushing are carried out for three different speeds and three different masses. For these analyses the maximum strain rates are analyzed and an empirical relation is derived between the actual crushing velocity and the strain rates in the bow structure.

Secondly, an analytical calculation procedure is presented which is based on a quasi-static simplified analytical calculation procedure modified by the derived relation between actual deformation velocity and the strain-rates. The varying crushing velocity is determined by an energy based procedure to give consistent estimates of the dynamic bow crushing forces.

Finally, the simulated numerical non-linear finite element dynamic and static crushing responses are compared with the results of the presented simplified analytical method.

The calculated results show considerable increase of the bow crushing force and energy absorption at elevated impact speeds. The dynamic effect is largest during the initial part of the impact and is then reduced as the kinetic energy is being absorbed and the impact speed goes to zero. That is, since the largest crushing deformation normally occurs at maximum displacement then the crushing force will not be influenced significantly by the strain rate effects. On the other hand the dynamic

effect in the initial impact phase results in much higher crushing forces at displacements where the contact area is still relatively small. Also the energy absorption for a given displacement increases significantly.

REFERENCES

Abramowicz W (1994). "Crushing Resistance of T, Y and X Sections," *MIT-Industry Joint Program on Tanker Safety, Massachusetts Institute of Technology, USA,* Report No. 24.

Amdahl J (1983)."Energy Absorption in Ship-Platform Impacts," phD Thesis. Report No. UR-83-34*, The Norwegian Institute of Technology, Trondheim.*

Cowper G. R. and Symonds P (1957). "Strain Hardening and Strain-Rate Effects in The Impact Loading of Cantilever Beams," Technical Report No. 28*, Division of Applied Mathematics, Brown University.*

Jones N (1989). Structural impact. *Cambridge, UK: Cambridge University Press.*

Lehmann E, Yu X (1995). "Progressive folding of bulbous bows," In*: The sixth international symposium on practical design of ship and mobile units (PRADS),* 2, 1048–1059.

Lützen M., Simonsen B.C. and Pedersen P.T. (2000). "Rapid Prediction of Damage to Struck and Striking Vessels in a Collision Event," *Proc. Ship Structure Symposium 2000, Society of Naval Architects and Marine Engineers, Washington D.C.*

Paik J.K., Pedersen P.T. (1995). "Ultimate and crushing strength of plated structures," *J Ship Res*,39(3):250–61.

Paik J.K. and Thayamballia. K (2003). "Ultimate Limit State Design of Steel-Plated Structures,"*Published by John Wiley & Sons Ltd, England*.

Pedersen P.T.,Valsgaard O.,Olsen D. and Spangenberg S. (1993). "Ship Impacts–Bow Collisions," *Int. J of Impact Engineering,* 13(2), 163-187.

Storheim M. and Amdahl J. (2015). "On the sensitivity to work hardening and strain-rate effects in non-linear FEM analysis of ship collisions," *Ships and Offshore Structures*. 13(2), 100-115.

Wang G (1995). "structure analysis of ships' collision and grounding," PhD thesis, *The university of Tokyo*.

Wierzbicki T, Abramowicz W (1983). "On the crushing mechanics of thin-walled structure," *J Appl Mech,* 50, 727–34.

Yamada Y. and Endo H. (2005). "Collapse Mechanism of the Buffer Bow Structure on Axial Crushing," *International Journal of Offshore and Polar Engineering*, 15(2), 147-154.

Yamada Y. and Pedersen P.T. (2008). "A Benchmark Study of Procedures for Analysis of Axial Crushing of Bulbous Bows," *Marine Structures*. 21(2-3), 257–293.

Yang P. D. C. and Caldwell J. B. (1988). "Collision Energy Absorption of Ship Bow Structures," *Int. J. Impact Engineering,* 7(2), 181-196.

Yoshitake A., Sato k., Hosoya Y. and Okita T. (1998). "Dynamic Tensile Properties and Impact Absorbed Energy of Hat Square Coloumn in Automotive Steel Sheets," *Japan NKK Technical*

Zhang S, Ocakli H, Pedersen P.T. (2004). "Crushing of Ship Bows in Head-on Collision,"*Int. J. Maritime Engineering,* 146(A2), 39-46. *Review,* 79.